Journals of Gerontology: BIOLOGICAL SCIENCES
Cite journal as: J Gerontol A Biol Sci Med Sci
doi:10.1093/gerona/glt078



# Variegated Expression of *Hsp22* Transgenic Reporters Indicates Cell-specific Patterns of Aging in *Drosophila* Oenocytes

John Tower, Gary Landis, Rebecca Gao, Albert Luan, Jonathan Lee, and Yuanyue Sun

Molecular and Computational Biology Program, Department of Biological Sciences, University of Southern California, Los Angeles.

Address correspondence to Molecular and Computational Biology Program, University of Southern California, 1050 Childs Way, RRI 201, Los Angeles, CA 90089-2910. Email: jtower@usc.edu

The cytoplasmic chaperone gene *Hsp70* and the mitochondrial chaperone gene *Hsp22* are upregulated during normal aging in *Drosophila* in tissue-general patterns. In addition, *Hsp22* reporters are dramatically upregulated during aging in a subset of the oenocytes (liver-like cells). *Hsp22* reporter expression varied dramatically between individual oenocytes and between groups of oenocytes located in adjacent body segments, and was negatively correlated with accumulation of age pigment, indicating cell-specific and cell-lineage-specific patterns of oenocyte aging. Conditional transgenic systems were used to express 88 transgenes to search for trans-regulators of the *Hsp70* and *Hsp22* reporters during aging. The *wingless* gene increased tissue-general upregulation of both *Hsp70* and *Hsp22* reporters. In contrast, the mitochondrial genes *MnSOD* and *Hsp22* increased expression of *Hsp22* reporters in the oenocytes and decreased accumulation of age pigment in these cells. The data suggest that cell-specific and cell lineage–specific patterns of mitochondrial malfunction contribute to oenocyte aging.

**Key Words:** Mitochondria—Age pigment—Mosaic—Cell lineage—Prepattern.

*Received February 4, 2013; Accepted April 19, 2013*

*Decision Editor: Rafael de Cabo, PhD*

IDENTIFYING biomarkers of aging that variegate between different individuals (1–5) and between different cells and tissues within an individual is of particular interest as it may help explain the large and apparently stochastic variation observed in life-span and aging phenotypes (6,7). The changes in gene expression that occur during normal aging in *Drosophila* are similar to an oxidative and proteotoxic stress response (1,8–11), including upregulated expression of the cytoplasmic chaperone Hsp70 (12) and the mitochondrial chaperone Hsp22 (13,14). Upregulation of *Hsp70* and *Hsp22* transgenes during aging requires functional heat shock factor (HSF)-binding sites (Heat Shock Elements, HSEs) in the gene promoters (13,15), consistent with activation of the unfolded protein response. The time course of Hsp gene upregulation during aging scales with life span as altered by temperature or oxidative stress (12). Moreover, the expression of *Hsp70-GFP* and *Hsp22-GFP* transgenic reporters in young individual flies is partially predictive of remaining life span (2), indicating that both these genes are biomarkers of *Drosophila* aging (16).

In addition to the common features of *Hsp70* and *Hsp22* expression, several results have suggested that *Hsp22* may have an additional regulatory input during aging (13). For example, *Hsp22* reporters exhibit a greater fold-induction when the fly is challenged with oxidative stress (1). In addition, *Hsp22* expression is increased during the first half of adult life in strains that have been genetically selected for increased life span (17). Finally, *MnSOD* overexpression can extend the life span of adult flies (18), and this is associated with increased expression of *Hsp22*, but not *Hsp70* (19). These observations prompted additional analysis of the regulation of *Hsp70* and *Hsp22* expression during aging.

The oenocytes are large, postmitotic, and metabolically active cells that appear similar to hepatocytes because they carry out liver-like lipid processing reactions. These reactions include ketogenesis during the fasting response in larvae (20) and synthesis of cuticular hydrocarbons in adults, including ones that mark species and sexual identity (21,22) and that change in composition and function during aging (23–25). The oenocytes derive their name from the Greek word for wine (*oenos*) because these cells dramatically accumulate dark-colored age pigment as a byproduct of cellular metabolic activity. Pigment accumulation during aging is also observed in mammalian tissues including the liver (26–28). The oenocytes are located in the abdomen of the fly, immediately beneath the translucent cuticle, and are arranged in clusters along the ventral midline and in a row along the dorsal side of each abdominal segment. The large size, characteristic arrangement, and age pigment accumulation facilitates the visualization of these cells in live flies. In this study, we report that *Drosophila* oenocytes display variegated expression of the aging biomarkers *Hsp22* and age pigment, indicating cell-specific and cell lineage–specific patterns of mitochondrial failure during aging.

## Methods

### *Drosophila* Culture and Strains

The *Hsp70-GFP*, *Hsp70-DsRED*, *Hsp22-GFP*, and *Hsp22-DsRED* reporter strains are as previously described (2), and the *Hsp22-LacZ* reporter strain and in situ beta-galactosidase assay are as previously described (13). The *Desat1-GAL4* driver lines were generously provided by J. Levine (21), and the *UAS-DsRED[A]* reporter line was obtained from Bloomington *Drosophila* Stock Center. The Tet-on system driver strain *w[1118]; rtTA(3)[E2]* and the Gene-Switch system driver strain *w[1118]; Act-GS[255B]* as well as conditions for use of the systems are as previously described (29). Strains containing multiple transgenes were generated by recombination and/or by appropriate crosses to double-balancer strains. Transgenic strains used in the genetic screen are listed in Supplementary Table S1.

### *Genetic Screen for Trans-regulators of Hsp Reporter Expression During Aging*

Each of the 88 transgenes screened was assayed for its effects on both *Hsp22-GFP* reporter expression and on *Hsp70-GFP* reporter expression, as follows. Each of 57 Tet-on system target transgenic strains was crossed to each of two Tet-on system "tester" strains: *w[1118]; Hsp22-GFP[1MI1], rtTA(3)[E2]/TM3 Sb* and *w[1118]; Hsp70-GFP[1MI2], rtTA(3)[E2]/TM3 Sb*. Each of 31 Gene-Switch system transgenic strains was crossed to each of two Gene-Switch system "tester" strains: *w[1118]; Act-GS[255B]; Hsp22-GFP[1MI1]/TM3 Sb* and *w[1118]; Act-GS[255B]; Hsp70-GFP[2MI4]/TM3 Sb*. From each cross, 160 progeny were scored that contained the three desired transgenes (the driver, the Hsp reporter, and the target for overexpression). From these 160 flies, 40 males were maintained minus drug, 40 males plus drug, 40 females minus drug, and 40 females plus drug; at a density of approximately 20 flies per vial. Flies were passaged to fresh positive/negative drug media three times per week and were scored by fluorescence microscopy at ages 7, 30, and 60 days. Crosses of the "tester" strains to the *w[1118]* strain were used to generate control cohorts containing the driver transgene and Hsp reporter, but no overexpressed transgene, and these flies were used for comparison to experimental crosses and to control for any possible effects of drug treatment. All crosses were conducted with the "tester" strains as the female parent, except for crosses involving transgenes on the *X* chromosome. Strains scored as positive were confirmed in repeat experiments, and results were quantified as described below.

### *Fluorescence Imaging and Quantification*

Fluorescent images and overlays were generated using live flies anesthetized with humidified $CO_2$ gas, and the Leica MZFLIII fluorescence stereomicroscope and Spot imaging software (2). Quantification of fluorescence in flies was performed using more than or equal to six flies per sample. Flies were photographed from a ventral angle, and mean fluorescence intensity was determined using Image J software; the eye and any portions of the body occluded by the wing were excluded from analysis. The mean and standard deviation were determined for each sample, and experimental and control samples were compared using unpaired, two-sided *t*-tests. Additional quantification of fly and oenocyte fluorescence was conducted using Green Fluorescent Protein (GFP) video analysis and FluoreScore software (30), and by counting the number of *Hsp22-GFP*-positive oenocyte sectors in cohorts of flies. To estimate in vivo superoxide levels, transgenic flies containing the *Hsp22-GFP[1MI1]* reporter were dissected at 60 days of age according to the procedure of Krupp and Levine (31) to generate abdominal walls with attached oenocytes and fat-body tissue. The fat-body was partly dissected away to reveal regions of the oenocytes, and the tissues were incubated for 30 minutes at 25°C in media containing 5-μm MitoSOX-Red dye (Invitrogen Life Technologies).

## Results

### *Hsp Reporters are Upregulated During Aging in Tissue-General Patterns*

The expression of the *Hsp22-GFP* and *Hsp70-GFP* reporters were examined in live, anesthetized flies at young age (6 day old) and old age (60 day old) (Figure 1). Both the *Hsp70-GFP* reporter (Figure 1A) and the *Hsp22-GFP* reporter (Figure 1B) were upregulated in tissue-general patterns, particularly muscle and nervous tissue, as previously observed (2), and this expression pattern was slightly greater in males than in females (Supplementary Figure S1).

### *Hsp22 Reporters Are Upregulated During Aging in the Oenocytes*

The *Hsp22-GFP* reporters were also found to be dramatically upregulated during aging in a subset of the oenocytes (Figure 1B; indicated with white arrow) and this pattern was not observed with multiple *Hsp70* reporters. Induction of *Hsp22* reporters in the oenocytes was slightly greater in females than in males (Supplementary Figure S1B; quantification in Supplementary Figure S5). *Hsp22-GFP* expression in oenocytes was absent in young flies (0–20 days) and first became apparent at approximately 20–30 days in a semirandom pattern involving individual oenocytes scattered throughout the abdomen (Figure 2B; Supplementary Figure S1B), as well as in groups of adjacent oenocytes; often all of the oenocytes in a row along one (or sometimes both) side of a (random) abdominal segment were positive (Figure 1B; see also Figure 2E and quantification in Supplementary Figure S5). The intensity of reporter expression continued to increase with age,

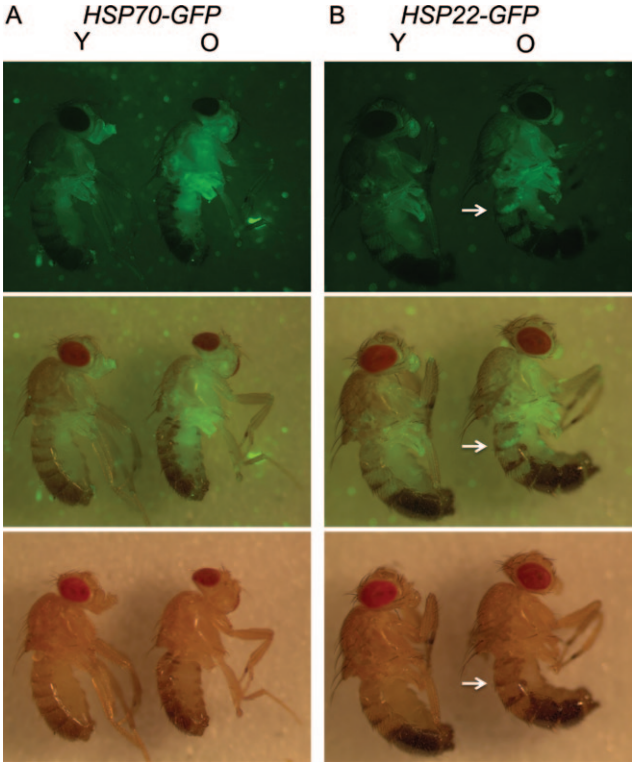


Figure 1. Increased expression of *Hsp70* and *Hsp22* reporters with age. Young (Y, 6 day old) and Old (O, 60 day old) male flies were analyzed by visible and fluorescence microscopy. The GFP image is shown in the top panels, the visible light image in the bottom panels, and the GFP/visible overlay in the middle panels. (**A**) *Hsp70-GFP* reporter, genotype *yw*; *Hsp70GFP[2MI4]/+*. (**B**) *Hsp22-GFP* reporter, genotype *yw*; *Hsp22-GFP[1MI1]/+*. Oenocytes with expression of the *Hsp22-GFP* reporter and correspondingly reduced age pigment are indicated by arrow.

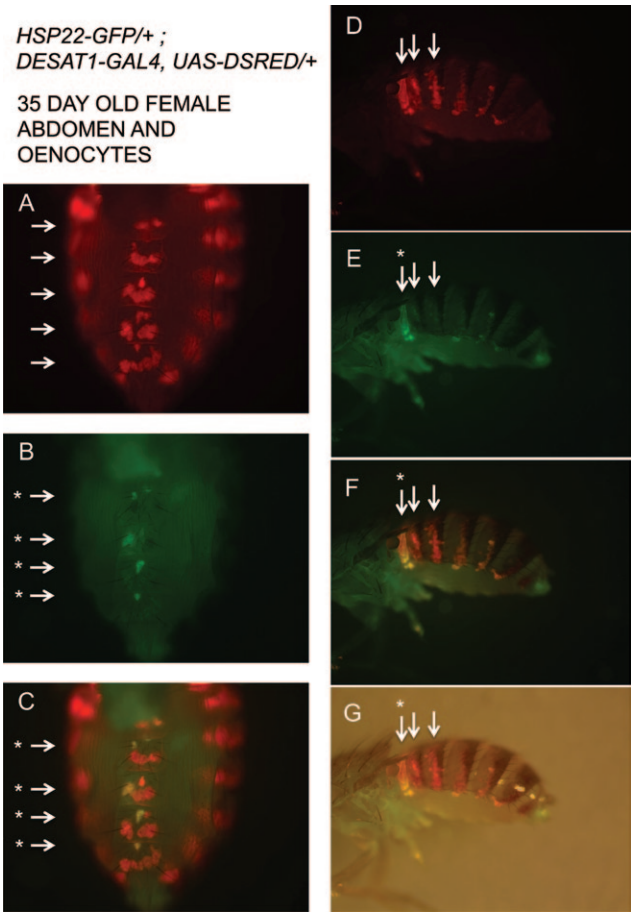


Figure 2. Variegated expression of *Hsp22-GFP* reporters in oenocytes. Female flies at 35 days of age were analyzed by fluorescence and visible light microscopy. Genotype *w[1118]; Hsp22-GFP[2MI4]/+; Desat1-Gal4[4M], UAS-DsRED[A]/+*. (**A–C**) Oenocyte clusters along the ventral midline (arrows). (**D–G**) Rows of oenocytes in the dorsal abdominal segments; the first three segments are in the plane of focus (arrows). (**A** and **D**) DsRED fluorescence marks all oenocytes (arrows). (**B** and **E**) *Hsp22-GFP* expression marks isolated oenocytes (**B**) and one row of oenocytes (**E**) in green (indicated by asterisk). (**C** and **F**) Overlay of DsRED and GFP images marks common cells as yellow (indicated by asterisk). (**G**) Overlay of visible light, DsRED, and GFP images.

and additional positive cells sometimes became apparent at later ages. The number of positive oenocytes varied greatly from fly-to-fly, and flies were never observed with all the oenocytes marked. Which oenocytes and which abdominal segment(s) were affected appeared to be random in males, whereas in females there was a slight preference for oenocytes located near the ventral midline of the most ventral segments (Supplementary Figure S1B, indicated with asterisk). When multiple oenocytes in an abdominal segment were marked, the oenocytes most distal to the dorsal midline (ie, at the end of the row of oenocytes) tended to have the greatest levels of expression (see Figures 1B, 2E and 4A). A similar pattern of expression was observed with additional independent transgenic lines of the *Hsp22-GFP* reporter and with multiple independent transgenic lines of the *Hsp22-DsRED* reporter (data not shown), as well as with *Hsp22-LacZ* reporter strains that contain more extensive *Hsp22* gene sequences (Supplementary Figure S2C), thereby demonstrating that expression of *Hsp22* reporters in a subset of the oenocytes is not simply a consequence of a particular chromosomal insertion site, construct design, or genetic background. The dramatic upregulation of *Hsp22* reporters in a subset of the oenocytes was unique to aging, as it was not observed upon acute induction of the *Hsp22* reporters with heat stress ([2] and additional data not shown).

### *Variegated Expression of Hsp22 Reporters by Cell and by Body Segment*

To confirm the identification of the *Hsp22-GFP*-positive cells as oenocytes, the oenocytes were specifically marked with Discosoma sp. red-fluorescent protein (DsRED) fluorescence by adding the oenocyte-specific driver construct *Desat1-GAL4* (21) and a *UAS-DsRED* reporter construct (Figure 2A). A ventral view of the abdomen is presented to highlight the clusters of oenocytes arranged along the ventral midline (arrows). Dramatic induction of the *Hsp22-GFP* reporter was observed in a subset of the oenocytes at age 35 days (Figure 2B, indicated with asterisks). Overlay

of the DsRED and GFP images reveals *Hsp22-GFP*-positive oenocytes in yellow color adjacent to oenocytes with no expression of *Hsp22-GFP* (Figure 2C), thereby demonstrating cell-specific patterns of *Hsp22* induction during aging in the oenocytes. Similarly, *Hsp22-GFP* induction often occurred in all of the oenocytes of one abdominal segment (Figure 2E, indicated with asterisk), whereas oenocytes in adjacent body segments remained largely or completely negative (arrows). Because the oenocytes in each abdominal segment represent a distinct developmental cell lineage (32–34), this pattern suggests cell lineage–specific induction of the *Hsp22* reporter in the oenocytes during aging.

### *A Genetic Screen for Trans-regulators of Hsp Gene Expression During Aging*

To further characterize the regulation of Hsp gene induction during aging, 88 transgenes (Supplementary Table S1) representing 57 genes were overexpressed specifically in adult flies in a tissue-general pattern. Overexpression was produced using the Tet-on and/or Gene-Switch conditional systems, in genetic backgrounds containing the *Hsp22-GFP* and *Hsp70-GFP* reporters, in cohorts of more than or equal to 160 flies for each transgene. Overexpression of *wingless* increased the tissue-general pattern of *Hsp70-GFP* and *Hsp22-GFP* reporter expression during aging (Figure 3A; Supplementary Figure S3), consistent with the ability of *wingless* overexpression in adult flies to dramatically decrease life span (35) and the implication of the *wingless* pathway in senescence pathways in other systems (36–38); although notably the oenocyte-specific induction of *Hsp22-GFP* during aging was not increased by *wingless* (Figure 3A and additional data not shown). None of the other transgenes tested had a detectable effect on the tissue-general expression pattern of the Hsp reporters, including several that dramatically decrease life span when overexpressed (eg, *ras-activated-form*, *doublesex-F*, *fruitless-MA*) (35,39) and several previously reported to have favorable effects on life span.

Two genes were found to dramatically increase the preferential expression of *Hsp22-GFP* reporters in the aging oenocytes: the mitochondrial gene *MnSOD* (also called *SOD2*; Figure 3B) and *Hsp22* itself (Supplementary Figure S4; quantification in Supplementary Figure S5). Both *MnSOD* overexpression and *Hsp22* overexpression increased the number of *Hsp22-GFP*-positive oenocytes, and appeared to increase the amount of *Hsp22-GFP* expression in each oenocyte, with relatively greater effects observed for *MnSOD*.

### *Hsp22 Reporter Expression Is Negatively Correlated With Accumulation of Age Pigment*

The accumulation of brown age pigment in the oenocytes is readily apparent by age 30 days (Supplementary Figure S2A) and continues to accumulate with advancing age (Figure 4A). The age pigment in the oenocytes did not

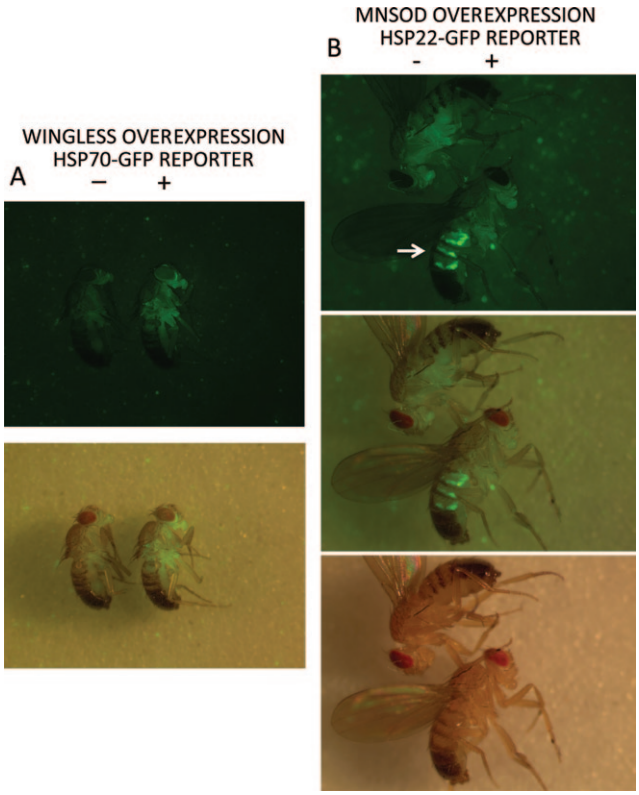


Figure 3. *Hsp-GFP* reporter trans-activation by *wingless* and *MnSOD*. (**A**) *wingless* overexpression. Flies bearing the *Hsp70-GFP* reporter were cultured in the absence (−) or presence (+) of RU486 drug to induce overexpression of *wingless* and were analyzed at age 60 days. Genotype *w[1118]; Act-GS[255B]/pUAS-wingless[3C]; Hsp70-GFP[2MI4]/+*. Whole-body GFP images are shown in the upper panel and GFP/visible light overlay images in the lower panel. (Quantification is presented in Supplementary Figure S3B). (**B**) *MnSOD* overexpression. Flies bearing the *Hsp22-GFP* reporter were cultured in the absence (−) or presence (+) of DOX drug to induce overexpression of *MnSOD* and were analyzed at age 60 days. Genotype *w[1118]; tetO-MnSOD[22]; Hsp22-GFP[1MI1], rtTA(3)[E2]/+*. Whole-body GFP images are shown in the upper panel, visible light images in the lower panel, and GFP/visible light overlay images in the middle panel. Arrow indicates *Hsp22-GFP* reporter expression in oenocytes.

fluoresce upon stimulation with 365 nm light, suggesting that it is chemically distinct from the fluorescent advanced-glycation end-products that accumulate with age in other tissues and are readily detected by fluorescence (Supplementary Figure S2B) (26,40). Strikingly, in every case, *Hsp22-GFP*-positive oenocytes had reduced accumulation of age pigment relative to *Hsp22-GFP*-negative oenocytes (Figure 4A). Oenocytes with reduced age pigment were also observed in old flies from additional laboratory and wild-type strains (data not shown), indicating that this variability in age pigment is not unique to a particular genetic background. In addition, both *MnSOD* and *Hsp22* overexpression dramatically decreased age pigment accumulation in the oenocytes (Figure 3B; Supplementary Figure S4). No other transgenes, including *Cu/ZnSOD*, were found to affect age pigment accumulation in the oenocytes, either positively or negatively. To rule

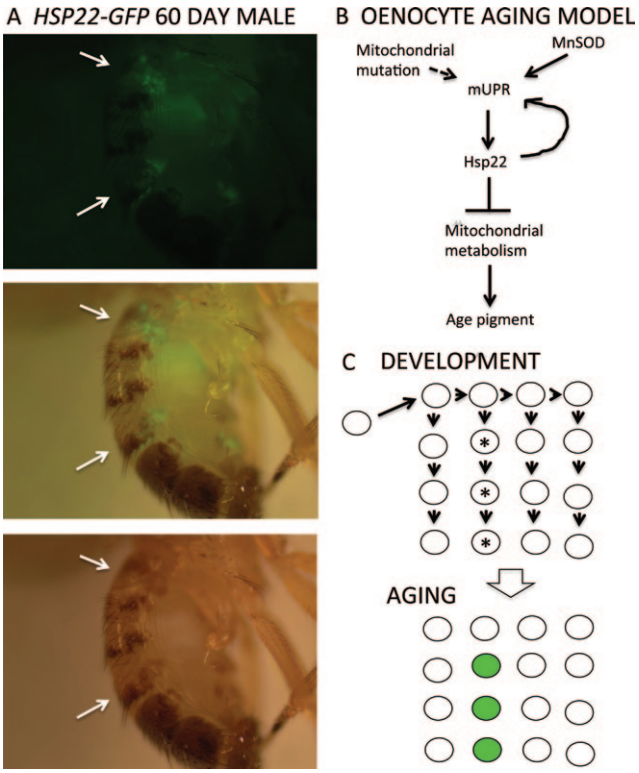


Figure 4. *Hsp22-GFP*-positive cells have reduced age pigment. (**A**) A 60-day-old male fly bearing the *Hsp22-GFP* reporter was analyzed by fluorescence and visible light microscopy. Genotype *yw; Hsp22-GFP[1MI1]*. The GFP image is shown in the top panel, the visible light image in the bottom panel, and the GFP/visible light overlay in the middle panel. Arrows indicate oenocytes with expression of the *Hsp22-GFP* reporter and reduced accumulation of age pigment. (**B** and **C**) Model for regulation of *Hsp22* expression in aging oenocytes. (**B**) Regulatory interactions suggested by this study and previous studies are indicated with solid arrows; hypothesized effect of mitochondrial mutation is indicated with dashed arrow. (**C**) During development of the animal, a mitochondrial mutation and/or bottleneck event (indicated with asterisk) is inherited by a particular oenocyte cell lineage; during aging this mitochondrial mutation leads to mitochondrial stress, *Hsp22* induction, reduced metabolism and reduced pigment accumulation.

out any possible effects of fluorescent protein expression on age pigment accumulation, both the Tet-on and GAL4/UAS systems were used to drive high-level expression of GFP and DsRED reporters in the oenocytes, and this had no detectable effect on age pigment; moreover, *MnSOD* overexpression decreased oenocyte age pigment in the absence of GFP expression (data not shown).

To investigate cellular levels of oxidative stress, abdominal wall tissues from 60-day-old flies containing the *Hsp22-GFP* reporter were stained with the superoxide indicator MitoSOX-Red dye (Supplementary Figure S2D–L). Fat-body tissue had relatively higher level signal, whereas oenocyte tissue had relatively lower level signal (Supplementary Figure S2D–F). *Hsp22-GFP*-positive oenocytes had no detectable enrichment for MitoSOX-Red staining (Supplementary Figure S2G–I), and often appeared to have reduced signal relative to adjacent *Hsp22-GFP*-negative oenocytes (Supplementary Figure S2J–L).

## Discussion

Both *Hsp70* and *Hsp22* transgenic reporters are upregulated during aging in tissue-general patterns and this pattern requires functional HSEs in the gene's promoters, consistent with activation through HSF and the cytoplasmic unfolded protein response (16). In addition, the *Hsp22* reporters were also dramatically upregulated during aging in a subset of the oenocytes in a cell-specific and cell lineage–specific pattern. This pattern suggests that the affected oenocytes are aging more quickly and/or differently than their neighbors. The number of positive oenocytes varied dramatically from fly-to-fly, and it will be of interest in the future to determine if this variation might correlate with individual animal life span. Because *Hsp22* encodes a mitochondrial chaperone (14) that is robustly induced in response to disrupted mitochondrial protein synthesis (41), and *Hsp22* reporter expression in the oenocytes was negatively correlated with the metabolic markers age pigment and superoxide, the data indicate cell-specific patterns of mitochondrial malfunction in the oenocytes during aging.

The results of the genetic screen further support the link between *Hsp22* expression, age pigment accumulation, and mitochondrial function during oenocyte aging. The *wingless* gene increased the tissue-general expression of the *Hsp70* and *Hsp22* reporters during aging, but did not increase the preferential expression of *Hsp22* reporters in the oenocytes. Similarly, overexpression of *dHSF* increases the tissue-general expression of *Hsp70* and *Hsp22*, but not the oenocyte expression pattern of *Hsp22* (unpublished observations). The oenocyte pattern of *Hsp22* expression was increased only by two mitochondrial genes, *MnSOD* and *Hsp22* itself, thereby supporting the link between *Hsp22* expression and mitochondrial function; moreover, both *MnSOD* and *Hsp22* overexpression correspondingly reduced oenocyte age pigment accumulation. Hsp22 localizes to the mitochondrial matrix (14); however, its specific targets in that compartment remain unknown. The negative correlation between *Hsp22-GFP* expression and markers of metabolic activity does not inform on cause and effect; however, one possibility is that Hsp22 and other components of the mitochondrial unfolded protein response act to repress mitochondrial metabolic activity and therefore reduce production of age pigment and superoxide (Figure 4B). Such a model is consistent with the observation that *MnSOD* overexpression induces *Hsp22* expression preferentially in the oenocytes (Figure 3B) and reduces adult fly metabolic activity (19).

Both *MnSOD* and *Hsp22* have either positive or negative effects on fly life span depending on the level, life cycle stage, and tissue-specificity of overexpression (16,29,42), and it is possible that the life span increases may involve hormetic effects of these genes on mitochondrial function. Consistent with this idea, when life span is extended by either *MnSOD* overexpression (19) or *Hsp22* overexpression (42), it is associated with increased expression of

mitochondrial genes that are normally downregulated during aging (1,8). Similarly, in *Caenorhabditis elegans*, tissue-general overexpression of the mitochondrial MnSOD gene *sod-2* increases life span through a mechanism dependent on the stress–response transcription factor DAF-16, which is a positive regulator of Hsp gene expression (43). Interestingly, manipulations that increase mammalian life span are often associated with changes in liver mitochondrial gene expression and morphology (44,45) supporting the importance of this tissue for aging phenotypes.

Mitochondrial malfunction is implicated in aging in several *Drosophila* tissues, including gut (46), muscle, and nervous tissue (47,48). One appealing model is that the consequences of mitochondrial malfunction are partly tissue specific, for example, a mitochondrial unfolded protein response and reduced metabolic activity in a subset of the oenocytes versus increased oxidative stress and a cytoplasmic unfolded protein response in muscle tissue (12,16,47,49,50). The tissue-general expression of *Hsp70-GFP* and *Hsp22-GFP* reporters was relatively greater in males (Supplementary Figure S1), whereas the oenocyte pattern for *Hsp22-GFP* was relatively greater in females, in two different control genetic backgrounds (Supplementary Figure S5). Sex-specific metabolism is common across species and may be particularly costly for aging (44,48,51–55), and therefore the fact that the oenocytes are especially sex dimorphic in their metabolism (21–25) may contribute to the observed mitochondrial failure. Investigating possible tissue-specific responses to mitochondrial malfunction will be an interesting area for further research.

The cell lineage patterns of *Hsp22* and age pigment observed in aging oenocytes suggest that mitochondrial failure is due, at least in part, to a change that is heritable at the cellular level and that occurs during the development of these postmitotic cells (Figure 4C). The alternative, and equally intriguing, explanation for such patterns is a non–cell autonomous mechanism wherein mitochondrial failure in one cell favors mitochondrial failure in adjacent cells (56,57). Although non–cell autonomy cannot be definitively ruled out at this time, the frequent observation of intensely positive cells in direct contact with completely negative cells tends to argue against such a model. The nature of a heritable change might be epigenetic, a nuclear mutation, or a mitochondrial mutation. We favor the idea of mitochondrial mutation for several reasons, including the high mutation rate of *Drosophila* mitochondrial genomes (58), and the increasing evidence from mammals for a developmentally produced load of mitochondrial mutations (59) that is subject to developmental bottlenecks (60) and that can expand during aging (61–63). Evidence for a change in mitochondrial DNA deletion frequency during *Drosophila* development and aging is mixed (64–66); however, those results may have been influenced by the use of mixed tissues, and point mutations have not yet been assayed. The *Drosophila* oenocytes should provide a tractable model system in which to further investigate mechanisms for cell-specific patterns of mitochondrial failure and aging.

## Supplementary Material

Supplementary material can be found at: http://biomedgerontology.oxfordjournals.org/

## Funding

This work was supported by a grant from the Department of Health and Human Services to J.T. (AG011833).

## References

1. Landis GN, Abdueva D, Skvortsov D, et al. Similar gene expression patterns characterize aging and oxidative stress in *Drosophila melanogaster*. *Proc Natl Acad Sci U S A*. 2004;101:7663–7668.
2. Yang J, Tower J. Expression of *hsp22* and *hsp70* transgenes is partially predictive of drosophila survival under normal and stress conditions. *J Gerontol A Biol Sci Med Sci*. 2009;64:828–838.
3. Rea SL, Wu D, Cypser JR, Vaupel JW, Johnson TE. A stress-sensitive reporter predicts longevity in isogenic populations of *Caenorhabditis elegans*. *Nat Genet*. 2005;37:894–898.
4. Pincus Z, Slack FJ. Developmental biomarkers of aging in *Caenorhabditis elegans*. *Dev Dyn*. 2010;239:1306–1314.
5. Herndon LA, Schmeissner PJ, Dudaronek JM, et al. Stochastic and genetic factors influence tissue-specific decline in ageing *C. elegans*. *Nature*. 2002;419:808–814.
6. Martin GM. Stochastic modulations of the pace and patterns of ageing: impacts on quasi-stochastic distributions of multiple geriatric pathologies. *Mech Ageing Dev*. 2012;133:107–111.
7. Kirkwood TB, Feder M, Finch CE, et al. What accounts for the wide variation in life span of genetically identical organisms reared in a constant environment? *Mech Ageing Dev*. 2005;126:439–443.
8. Landis G, Shen J, Tower J. Gene expression changes in response to aging compared to heat stress, oxidative stress and ionizing radiation in Drosophila melanogaster. *Aging*. 2012;4:768–789.
9. Zou S, Meadows S, Sharp L, Jan LY, Jan YN. Genome-wide study of aging and oxidative stress response in *Drosophila melanogaster*. *Proc Natl Acad Sci U S A*. 2000;97:13726–13731.
10. Pletcher SD, Macdonald SJ, Marguerie R, et al. Genome-wide transcript profiles in aging and calorically restricted *Drosophila melanogaster*. *Curr Biol*. 2002;12:712–723.
11. Zhan M, Yamaza H, Sun Y, Sinclair J, Li H, Zou S. Temporal and spatial transcriptional profiles of aging in *Drosophila melanogaster*. *Genome Res*. 2007;17:1236–1243.
12. Wheeler JC, Bieschke ET, Tower J. Muscle-specific expression of *Drosophila* hsp70 in response to aging and oxidative stress. *Proc Natl Acad Sci U S A*. 1995;92:10408–10412.
13. King V, Tower J. Aging-specific expression of *Drosophila* hsp22. *Dev Biol*. 1999;207:107–118.
14. Morrow G, Inaguma Y, Kato K, Tanguay RM. The small heat shock protein Hsp22 of *Drosophila melanogaster* is a mitochondrial protein displaying oligomeric organization. *J Biol Chem*. 2000;275:31204–31210.
15. Wheeler JC, King V, Tower J. Sequence requirements for upregulated expression of *Drosophila* hsp70 transgenes during aging. *Neurobiol Aging*. 1999;20:545–553.
16. Tower J. Heat shock proteins and *Drosophila* aging. *Exp Gerontol*. 2011;46:355–362.
17. Kurapati R, Passananti HB, Rose MR, Tower J. Increased hsp22 RNA levels in *Drosophila* lines genetically selected for increased longevity. *J Gerontol A Biol Sci Med Sci*. 2000;55:B552–B559.
18. Sun J, Folk D, Bradley TJ, Tower J. Induced overexpression of mitochondrial Mn-superoxide dismutase extends the life span of adult *Drosophila melanogaster*. *Genetics*. 2002;161:661–672.
19. Curtis C, Landis GN, Folk D, et al. Transcriptional profiling of MnSOD-mediated lifespan extension in *Drosophila* reveals a species-general network of aging and metabolic genes. *Genome Biol*. 2007;8:R262.

20. Gutierrez E, Wiggins D, Fielding B, Gould AP. Specialized hepatocyte-like cells regulate *Drosophila* lipid metabolism. *Nature*. 2007;445:275–280.
21. Billeter JC, Atallah J, Krupp JJ, Millar JG, Levine JD. Specialized cells tag sexual and species identity in *Drosophila melanogaster*. *Nature*. 2009;461:987–991.
22. Shirangi TR, Dufour HD, Williams TM, Carroll SB. Rapid evolution of sex pheromone-producing enzyme expression in *Drosophila*. *PLoS Biol*. 2009;7:e1000168.
23. Fedina TY, Kuo TH, Dreisewerd K, Dierick HA, Yew JY, Pletcher SD. Dietary effects on cuticular hydrocarbons and sexual attractiveness in *Drosophila*. *PLoS One*. 2012;7:e49799.
24. Kuo TH, Yew JY, Fedina TY, Dreisewerd K, Dierick HA, Pletcher SD. Aging modulates cuticular hydrocarbons and sexual attractiveness in Drosophila melanogaster. *J Exp Biol*. 2012;215:814–821.
25. Kuo TH, Fedina TY, Hansen I, et al. Insulin signaling mediates sexual attractiveness in Drosophila. *PLoS Genet*. 2012;8:e1002684.
26. Jung T, Höhn A, Grune T. Lipofuscin: detection and quantification by microscopic techniques. *Methods Mol Biol*. 2010;594:173–193.
27. Yin D. Biochemical basis of lipofuscin, ceroid, and age pigment-like fluorophores. *Free Radic Biol Med*. 1996;21:871–888.
28. Schmucker DL, Sachs H. Quantifying dense bodies and lipofuscin during aging: a morphologist's perspective. *Arch Gerontol Geriatr*. 2002;34:249–261.
29. Ford D, Hoe N, Landis GN, et al. Alteration of Drosophila life span using conditional, tissue-specific expression of transgenes triggered by doxycyline or RU486/Mifepristone. *Exp Gerontol*. 2007;42:483–497.
30. Ardekani R, Huang YM, Sancheti P, Stanciauskas R, Tavaré S, Tower J. Using GFP video to track 3D movement and conditional gene expression in free-moving flies. *PLoS One*. 2012;7:e40506.
31. Krupp JJ, Levine JD. Dissection of oenocytes from adult Drosophila melanogaster. *J Vis Exp*. 2010;41:2242.
32. Lawrence PA, Johnston P. Cell lineage of the *Drosophila* abdomen: the epidermis, oenocytes and ventral muscles. *J Embryol Exp Morphol*. 1982;72:197–208.
33. Lawrence PA, Johnston P. Observations on cell lineage of internal organs of *Drosophila*. *J Embryol Exp Morphol*. 1986;91:251–266.
34. Gould AP, Elstob PR, Brodu V. Insect oenocytes: a model system for studying cell-fate specification by Hox genes. *J Anat*. 2001;199:25–33.
35. Shen J, Curtis C, Tavaré S, Tower J. A screen of apoptosis and senescence regulatory genes for life span effects when over-expressed in *Drosophila*. *Aging (Albany NY)*. 2009;1:191–211.
36. DeCarolis NA, Wharton KA Jr, Eisch AJ. Which way does the Wnt blow? Exploring the duality of canonical Wnt signaling on cellular aging. *Bioessays*. 2008;30:102–106.
37. Conboy IM, Rando TA. Heterochronic parabiosis for the study of the effects of aging on stem cells and their niches. *Cell Cycle*. 2012;11:2260–2267.
38. Naito AT, Shiojima I, Komuro I. Wnt signaling and aging-related heart disorders. *Circ Res*. 2010;107:1295–1303.
39. Shen J, Ford D, Landis GN, Tower J. Identifying sexual differentiation genes that affect *Drosophila* life span. *BMC Geriatr*. 2009;9:56.
40. Jacobson J, Lambert AJ, Portero-Otín M, et al. Biomarkers of aging in *Drosophila*. *Aging Cell*. 2010;9:466–477.
41. Chen S, Oliveira MT, Sanz A, et al. A cytoplasmic suppressor of a nuclear mutation affecting mitochondrial functions in *Drosophila*. *Genetics*. 2012;192:483–493.
42. Kim HJ, Morrow G, Westwood JT, Michaud S, Tanguay RM. Gene expression profiling implicates OXPHOS complexes in lifespan extension of flies over-expressing a small mitochondrial chaperone, Hsp22. *Exp Gerontol*. 2010;45:611–620.
43. Cabreiro F, Ackerman D, Doonan R, et al. Increased life span from overexpression of superoxide dismutase in *Caenorhabditis elegans* is not caused by decreased oxidative damage. *Free Radic Biol Med*. 2011;51:1575–1582.
44. Amador-Noguez D, Zimmerman J, Venable S, Darlington G. Gender-specific alterations in gene expression and loss of liver sexual dimorphism in the long-lived Ames dwarf mice. *Biochem Biophys Res Commun*. 2005;332:1086–1100.
45. Khraiwesh H, Lopez-Dominguez JA, Lopez-Lluch G, et al. Alterations of ultrastructural and fission/fusion markers in hepatocyte mitochondria from mice following calorie restriction with different dietary fats. *J Gerontol A Biol Sci Med Sci*. 2013; Feb 12 [Epub ahead of print]. doi:10.1093/gerona/glt006.
46. Rera M, Bahadorani S, Cho J, et al. Modulation of longevity and tissue homeostasis by the Drosophila PGC-1 homolog. *Cell Metab*. 2011;14:623–634.
47. Cho J, Hur JH, Walker DW. The role of mitochondria in *Drosophila* aging. *Exp Gerontol*. 2011;46:331–334.
48. Tower J. Sex-specific regulation of aging and apoptosis. *Mech Ageing Dev*. 2006;127:705–718.
49. Demontis F, Perrimon N. FOXO/4E-BP signaling in *Drosophila* muscles regulates organism-wide proteostasis during aging. *Cell*. 2010;143:813–825.
50. Augustin H, Partridge L. Invertebrate models of age-related muscle degeneration. *Biochim Biophys Acta*. 2009;1790:1084–1094.
51. Cortright RN, Koves TR. Sex differences in substrate metabolism and energy homeostasis. *Can J Appl Physiol*. 2000;25:288–311.
52. Bonduriansky R, Chenoweth SF. Intralocus sexual conflict. *Trends Ecol Evol*. 2009;24:280–288.
53. Magwire MM, Yamamoto A, Carbone MA, et al. Quantitative and molecular genetic analyses of mutations increasing *Drosophila* life span. *PLoS Genet*. 2010;6:e1001037.
54. Liu D, Sartor MA, Nader GA, et al. Microarray analysis reveals novel features of the muscle aging process in men and women. *J Gerontol A Biol Sci Med Sci*. 2013; Feb 15 [Epub ahead of print]. doi:10.1093/gerona/glt015.
55. Hughes BG, Hekimi S. A mild impairment of mitochondrial electron transport has sex-specific effects on lifespan and aging in mice. *PLoS One*. 2011;6:e26116.
56. Nunnari J, Suomalainen A. Mitochondria: in sickness and in health. *Cell*. 2012;148:1145–1159.
57. Durieux J, Wolff S, Dillin A. The cell-non-autonomous nature of electron transport chain-mediated longevity. *Cell*. 2011;144:79–91.
58. Haag-Liautard C, Coffey N, Houle D, Lynch M, Charlesworth B, Keightley PD. Direct estimation of the mitochondrial DNA mutation rate in *Drosophila melanogaster*. *PLoS Biol*. 2008;6:e204.
59. Ameur A, Stewart JB, Freyer C, et al. Ultra-deep sequencing of mouse mitochondrial DNA: mutational patterns and their origins. *PLoS Genet*. 2011;7:e1002028.
60. Jokinen R, Junnila H, Battersby BJ. Gimap3: a foot-in-the-door to tissue-specific regulation of mitochondrial DNA genetics. *Small GTPases*. 2011;2:31–35.
61. Meissner C. Mutations of mitochondrial DNA: cause or consequence of the ageing process? *Z Gerontol Geriatr*. 2007;40:325–333.
62. Herbst A, Pak JW, McKenzie D, Bua E, Bassiouni M, Aiken JM. Accumulation of mitochondrial DNA deletion mutations in aged muscle fibers: evidence for a causal role in muscle fiber loss. *J Gerontol A Biol Sci Med Sci*. 2007;62:235–245.
63. Jarrett SG, Lewin AS, Boulton ME. The importance of mitochondria in age-related and inherited eye disorders. *Ophthalmic Res*. 2010;44:179–190.
64. Yui R, Matsuura ET. Detection of deletions flanked by short direct repeats in mitochondrial DNA of aging Drosophila. *Mutat Res*. 2006;594:155–161.
65. Chen X, Simonetti S, Di Mauro S, Schon EA. Accumulation of mitochondrial DNA deletions in organisms with various lifespans. *Bull Mol Biol Med*. 1993;18:57–66.
66. Schwarze SR, Weindruch R, Aiken JM. Decreased mitochondrial RNA levels without accumulation of mitochondrial DNA deletions in aging *Drosophila melanogaster*. *Mutat Res*. 1998;382:99–107.

**Variegated Expression of *Hsp22* Transgenic Reporters Indicates Cell-Specific Patterns of Aging in *Drosophila* Oenocytes**

John Tower, Gary Landis, Rebecca Gao, Albert Luan, Jonathan Lee, Yuanyue Sun

## SUPPLEMENTAL INFORMATION

## SUPPLEMENTAL METHODS

Tet-on system transgenic strains are as described in (1-8). Gene-Switch system transgenic strains were obtained from Bloomington *Drosophila* stock center, Harvard *Drosophila* stock center and VDRC as indicated in Supplemental Table S1, EcR strains are as described in (9), *fru* and *dsx* lines were provided by Michelle Arbeitman (10), *l(2)efl* line by H. Jasper (11).

**Supplemental Table S1.** List of all transgenic lines screened.

| Tet-on Gene Name | Type | Stock ID | Genotype |
|---|---|---|---|
| a | OE | | y-ac-w;P{PdL}a[3M1-67-3](2)/ CyO |
| α-Man-II | OE | | y-ac-w; P{PdL}a-Man-II[19B3](3)/TM3 |
| ash1 | OE | | y-ac-w;P{PdL}ash1[11A3](3) |
| beg | OE | | y-ac-w;P{PdL}beg CG7842[8-100-2](3) e[11] |
| beg | OE | | y-ac-w;P{PdL}beg CG7842[15-39-1](3) e[11]/TM3 |
| beg | OE | | y-ac-w;P{PdL}beg CG7842[13-115-4](3) e[11]/TM3 |
| Cct1 | OE | | y-ac-w;P{PdL}Cct1[8R128](3) e[11] |
| CG13012 | OE | | y-ac-w P{PdL}CG13012[3M1-8-3](1) |
| CG15160 | OE | | y-ac-w;P{PdL}CG15160[11-24-3](3) e[11] /TM3 |
| CG2127 | OE | | y-ac-w;P{PdL}CG2127[3M1-41](2)/ CyO |
| CG2909 | OE | | y-ac-w P{PdL}CG2909[13-2-1](1) |
| CG32188 | OE | | y-ac-w;P{PdL}CG33188[14-59-1A](3) e[11] |
| cher | OE | | y-ac-w;P{PdL}cher[8S64](3) e[11] |
| ckd | OE | | y-ac-w; P{PdL} ckd CG14959 YSL-17 (3) |
| ckd | OE | | y-ac-w; P{PdL} ckd CG14959 YSL-18 (3) |
| ckd | OE | | y-ac-w; P{PdL} ckd CG14959 YSL-46 (3) |
| ckd | OE | | y-ac-w;P{PdL}ckd CG14959[1M1-3-1](3) e[11] |

| | | |
|---|---|---|
| | | /TM3 |
| Crc | OE | y-ac-w;P{PdL}Crc[5M1-75-2](3) e[11] |
| dbr | OE | y-ac-w;P{PdL}dbr[2M1-81-1](2) |
| dbr | OE | y-ac-w;P{PdL}dbr[3M1-75-3](2) |
| demeter | OE | y-ac-w; P{PdL} demeter YSL-32 (3) |
| dve | OE | y-ac-w; P{PdL} dve YSL-45 (2) |
| edl | OE | y-ac-w;P{PdL}edl[4M1-27-3](2) |
| edl | OE | y-ac-w;P{PdL}edl[9-118-1](3) e[11] /TM3 |
| eIF3-S10 | OE | y-ac-w;P{PdL}eIF3-S10[8-56-2](3) e[11]/TM3 |
| enc | OE | y-ac-w;P{PdL}enc[3E36] (3) e[11] |
| foxo | OE | y-ac-w;P{PdL}foxo[Y2-26-3](3) e[11] /TM3 |
| fwd | OE | y-ac-w;P{PdL}fwd[8S25](3) e[11] |
| fz3 | OE | y-ac-w P{PdL}CG16785 fz3[1M1-59-4](1) |
| hairy | OE | y-ac-w; P{PdL} hairy YSL-1 (3) |
| hebe | OE | y-ac-w; P{hebe}DX2 (2) |
| hebe | OE | y-ac-w; P{hebe}AX (3) |
| hebe | OE | y-ac-w; P{PdL} hebe YSL-27 (2) |
| Hsp22 | OE | w;USC22 S(3)22A <++> |
| Hsp22 | OE | w;USC22 S(2)23 <+> |
| Hsp22 | OE | w;USC22 S(2)26 <++> |
| hUbb | OE (human) | w;Hubb(2)70 |
| javelin-like | OE | y-ac-w;P{PdL}CG3563[11-65-3-2](3) e[11] |
| lilli | OE | y-ac-w;P{PdL}lilli[5M1-53-3](2) /CyO |
| magu | OE | y-ac-w; P{magu}67-1 (3) |
| magu | OE | y-ac-w;P{magu}102 (3) |
| magu | OE | y-ac-w; P{PdL} magu YSL-3 (2) |
| MRG-15 | RNAi | w[1118]; p{RNAi DmMrg15}[53] (2) |
| numb | OE | y-ac-w; P{PdL} numb YSL-48 (2) |
| osa | OE | y-ac-w;P{PdL}osa[7M1-13-1](3) e[11] /TM3 |
| peg | OE | y-ac-w;P{PdL}peg CG8583[9-37-2](3) e[11] /TM3 |
| pter | OE | y-ac-w;P{PdL}pter CG3957[2-4-2-new](2) |
| pum | OE | y-ac-w;P{PdL}pum[3B2](3) |
| sima | OE | y-ac-w;P{PdL}similar[7M1-79-1](3) e[11] |
| Sod1 | OE | y-ac-w; P{*CuZnSOD*} [10], P{*CuZnSOD*}[21] (2) [B] |
| Sod2 | OE | y-ac-w; P{*MnSOD*} [22] <++> |
| Sod2 | OE | y-ac-w; P{*MnSOD*} [12] <++> |
| Sug | OE | y-ac-w;P{PdL}Sug[2C33](3) e[11] /TM3 |
| Tfb1 | OE | y-ac-w;P{PdL}Tfb1[8-49-4](2) |
| tincar | OE | y-ac-w;P{PdL}CG31246[1-25-4](3) e[11] /TM3 |
| veil | OE | y-ac-w;P{PdL}veil CG4827[5M1-12-2](3) e[11] /TM3 |
| VhaSFD | OE | y-ac-w;P{PdL}VhaSFD[4G14](2) /SM5 Cy |

**Geneswitch**

| Gene Name | Type | Stock ID | Genotype |
|---|---|---|---|
| 4EBP | OE | Bl#24854 | w[*]; P{w[+mC]=UAS-Thor.LL}s/TM6C, cu[1] Sb[1] |
| Atg8a | OE | Bl#10107 | w[1118]; P{w[+mC]=EP}Atg8a[EP362] |
| dsx[M] | OE | | w; P{UAS-dsx[M]}; + |
| EcR | OE (DN) | Bl#9451 | w[*]; P{w[+mC]=UAS-EcR.A.W650A}TP5 |
| EcR | OE (DN) | Bl#6869 | w[1118]; P{w[+mC]=UAS-EcR.B1-DeltaC655.F645A}TP1 |
| EcR | RNAi | | w[1118]; P{w[+mC]=UAS-EcR-RNAi}97 |
| EcR | OE | Bl#6470 | w[*]; P{w[+mC]=UAS-EcR.A}3a |
| EcR | OE | Bl#6469 | w[*]; P{w[+mC]=UAS-EcR.B1}3b |
| foxo | OE | Bl#9575 | y[1] w[*]; P{w[+mC]=UAS-foxo.P}2 |
| foxo | OE | Bl#21215 | y[1] w[67c23]; P{w[+mC] y[+mDint2]=EPgy2}foxo[EY16506] |
| fru | OE | | y w; P{UAS-fruMA}[7]; + |
| Hsp22 | OE | d07618 | P(12)Hsp22[d07618] <+> |
| Hsp22 | OE | d00797 | P(12)Hsp22[d00797] |
| Hsp22 | OE | Bl#20055 | y[1] w[67c23]; P{w[+mC] y[+mDint2]=EPgy2}Hsp22[EY09909] Hsp67Bb[EY09909] <+> |
| msn | OE | Bl#20015 | y[1] w[67c23]; P{w[+mC] y[+mDint2]=EPgy2}msn[EY08051]/TM3 |
| Hsp68 | OE | Bl#14806 | w[*]; P{w[+mC] y[+mDint2]=EPgy2}EY00050 |
| Hsp68 | OE | Bl#30109 | w[1118]; P{w[+mC]=EP}Hsp68[G4992] |
| Hsp70Aa | OE | Bl#17624 | y[1] w[67c23]; P{w[+mC] y[+mDint2]=EPgy2}Hsp70Aa[EY09953] |
| Hsp70Ab | OE | Bl#15327 | y[1] w[67c23]; P{w[+mC] y[+mDint2]=EPgy2}Hsp70Ab[EY01148] |
| l(2)efl | OE | | w[1118]; pUAST-l(2)efl |
| p53 | OE | Bl#9570 | w[1118]; P{w[+mC]=UAS-p53.Ex}2 |
| p53[259H] | OE (DN) | Bl#6582 | w[1118]; P{w[+mC]=GUS-p53.259H}3.1 |
| p53[H159N] | OE (DN) | Bl#8420 | y[1] w[1118]; P{w[+mC]=UAS-p53.H159N.Ex}2 |
| RAS85D | OE (AF) | Bl#4847 | w1118; +; P{UAS-Ras85D.V12}TL1 |
| Tor | OE | Bl#7012 | y[1] w[*] P{ry[+t7.2]=hsFLP}1; P{w[+mC]=UAS-Tor.WT}III |
| Tor[DN] | OE (DN) | Bl#7013 | y[1] w[*]; P{w[+mC]=UAS-Tor.TED}II |
| tra | OE | Bl#4590 | w[1118]; P{w[+mC]=UAS-tra.F}20J7 |
| wg | OE | Bl#5919 | w*; P{UAS-wg.H.T:HA1}3C;+ <++> |
| wg | OE | Bl#5918 | w*; +; P{UAS-wg.H.T:HA1}6C <+> |
| wg | RNAi | VDRC 13351 | w[1118]; P{GD5007}v13351 |
| wg | RNAi | VDRC 13352 | w[1118]; P{GD5007}v13352 |

Bl=Bloomington, d=Harvard, VDRC=Vienna, OE = over-expression, DN = dominant negative, AF= active form, <++> = higher activity, <+> = lower activity

## SUPPLEMENTAL REFERENCES


1. Landis G, Bhole D, Lu L, Tower J. High-frequency generation of conditional mutations affecting *Drosophila melanogaster* development and life span. Genetics. 2001;158:1167-1176.
2. Landis GN, Bhole D, Tower J. A search for doxycycline-dependent mutations that increase *Drosophila melanogaster* life span identifies the *VhaSFD, Sugar baby, filamin, fwd* and *Cctl* genes. Genome Biol. 2003;4:R8.
3. Hoe N, Huang CM, Landis G*, et al.* Ubiquitin over-expression phenotypes and *ubiquitin* gene molecular misreading during aging in *Drosophila melanogaster*. Aging (Albany NY). 2011;3:237-261.
4. Bhole D, Allikian MJ, Tower J. Doxycycline-regulated over-expression of hsp22 has negative effects on stress resistance and life span in adult *Drosophila melanogaster.* Mech Ageing Dev. 2004;125:651-663.
5. Ford D, Hoe N, Landis GN*, et al.* Alteration of *Drosophila* life span using conditional, tissue-specific expression of transgenes triggered by doxycyline or RU486/Mifepristone. Exp Gerontol. 2007;42:483-497.
6. Li Y, Tower J. Adult-specific over-expression of the *Drosophila* genes *magu* and *hebe* increases life span and modulates late-age female fecundity. Molecular genetics and genomics : MGG. 2009;281:147-162.
7. Khokhar A, Chen N, Yuan JP*, et al.* Conditional switches for extracellular matrix patterning in *Drosophila melanogaster*. Genetics. 2008;178:1283-1293.
8. Zhang H, Li Y, Yang J, Tominaga K, Pereira-Smith OM, Tower J. Conditional inactivation of MRG15 gene function limits survival during larval and adult stages of *Drosophila melanogaster*. Exp Gerontol. 2010;45:825-833.
9. Roignant JY, Carre C, Mugat B, Szymczak D, Lepesant JA, Antoniewski C. Absence of transitive and systemic pathways allows cell-specific and isoform-specific RNAi in *Drosophila*. Rna. 2003;9:299-308.
10. Sanders LE, Arbeitman MN. Doublesex establishes sexual dimorphism in the *Drosophila* central nervous system in an isoform-dependent manner by directing cell number. Dev Biol. 2008;320:378-390.
11. Wang MC, Bohmann D, Jasper H. JNK extends life span and limits growth by antagonizing cellular and organism-wide responses to insulin signaling. Cell. 2005;121:115-125.


## SUPPLEMENTAL FIGURE LEGENDS

**Supplemental Figure S1.** Quantification of *Hsp70* and *Hsp22* reporters in males and females. The *Hsp70-GFP* reporter (**A**), and the *Hsp22-GFP* reporter (**B**), were analyzed in male (M) and female (F) flies, as indicated, at age 60 days. GFP fluorescence is shown

in upper panels, and visible light/GFP overlay in the lower panels; exposure times were limited to highlight differences between male and female. (**A**) Genotype *yw;Hsp70-GFP[2MI4]/+*. (**B**) Genotype *yw; Hsp22-GFP[1MI1]/+*. Expression of the Hsp22-GFP reporter in oenocytes was generally more extensive in females than in males, and is indicated with white arrows (quantification presented in Supplemental Figure S5). (**C**) GFP was quantified using Image J software in groups of 6 flies for each sample, as indicated. Mean and standard deviation are plotted, and the data for females was compared to males using unpaired, two-sided t-tests, and statistically significant differences ($p < 0.05$) are indicated with asterisk.

**Supplemental Figure S2.** Oenocyte marker characterization. (**A**) Male flies were photographed using visible light at ages 6 days and 30 days, as indicated. Arrow indicates age pigment accumulation in oenocytes. Genotype wild-type (Oregon R strain). (**B**) Male flies were photographed at ages 6 days and 60 days, as indicated, using visible (white) light illumination and using 365nm light illumination, and the visible light/fluoresecence image overlay is presented. Increased bluish-lavender fluorescence in the old fly head, thorax and abdomen is indicated with white arrows; no fluorescence was detected from oenocytes. Genotype wild-type (Oregon R strain). (**C**) Expression of *Hsp22-LacZ* reporter in oenocytes. Dissected abdomens from 6 day old and 30 day old flies were stained for beta-galactosidase activity. Arrow indicates reporter expression in oenocytes in one abdominal segment. Genotype *w[1118]; Hsp22-LacZ[3A]*. (**D-L**) Tissue staining with MitoSOX-red dye. Flies at 60 days of age containing the *Hsp22-GFP* reporter were dissected and the tissues stained with MitoSOX-Red dye to indicate superoxide levels. (**D-F**) Dorsal view of dissected abdominal wall, with oenocytes attached (arrows) and partial fat-body tissue attached (asterisk). The posterior of the abdomen is to the left and anterior is to the right. (**G-L**) Individual abdominal segments were dissected with oenocytes attached (arrows) and partial fat-body tissue attached (asterisks). (**D, G, J**) GFP fluorescence imaging of oenocytes with high-level expression of *Hsp22-GFP* reporter (arrows). (**E, H, K**) Flourescence imaging of MitoSOX-Red staining. Fat-body tissue had relatively higher-level signal and is indicated with asterisks.

Oenocytes had relatively lower-level signal and are indicated with arrows. (**F, I, L**) Overlay of *Hsp22-GFP* and MitoSOX-red images.

**Supplemental Figure S3**. Quantification of *Hsp22-GFP* reporter induction in oenocytes with over-expression of *MnSOD* and *Hsp22*. (**A**) Sector numbering. Groups ("Sectors") of oenocytes in each segment and along the midline were numbered as indicated. A sector containing one or more intensely positive cells was counted as positive. (**B**) *MnSOD* over-expression. Male and female flies containing the *Hsp22-GFP* reporter, and either no target transgene (Control) or the *tetO-MnSOD[12]* transgene or the *tetO-MnSOD[22]* transgene, were cultured in the absence (-) and presence (+) of drug to age 60 days, as indicated. (**C**) *Hsp22* over-expression. Male and female flies containing the *Hsp22-GFP* reporter, and either no target transgene (Control) or the *tetO-Hsp22[26]* transgene, the *tetO-Hsp22[22A]* transgene, or the *tetO-Hsp22[23]* transgene were cultured in the absence (-) and presence (+) of drug to age 60 days, as indicated. The number of GFP-positive groups of oenocytes was counted in cohorts of 35 flies for each sample and plotted. The mean value is indicated with a red line, and (+) was compared to (-) for each genotype using Mann-Whitney test, and statistically significant differences are indicated with an asterisk. Note that the greater degree of trans-activation apparent in males relative to females is believed to be due in part to the fact that the *rtTA(3)E2* driver has ~50% greater activity in males than in females (data not shown).

A Hsp70-GFP

M F

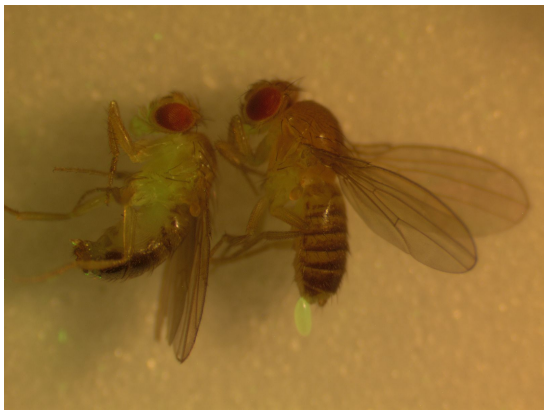

B Hsp22-GFP

M F

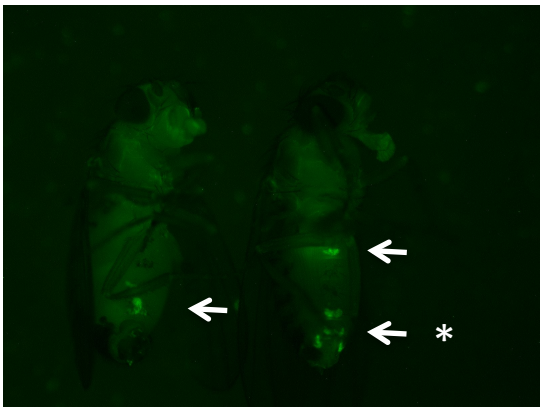


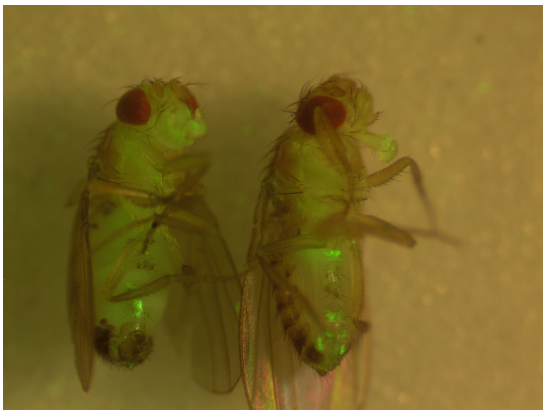

C

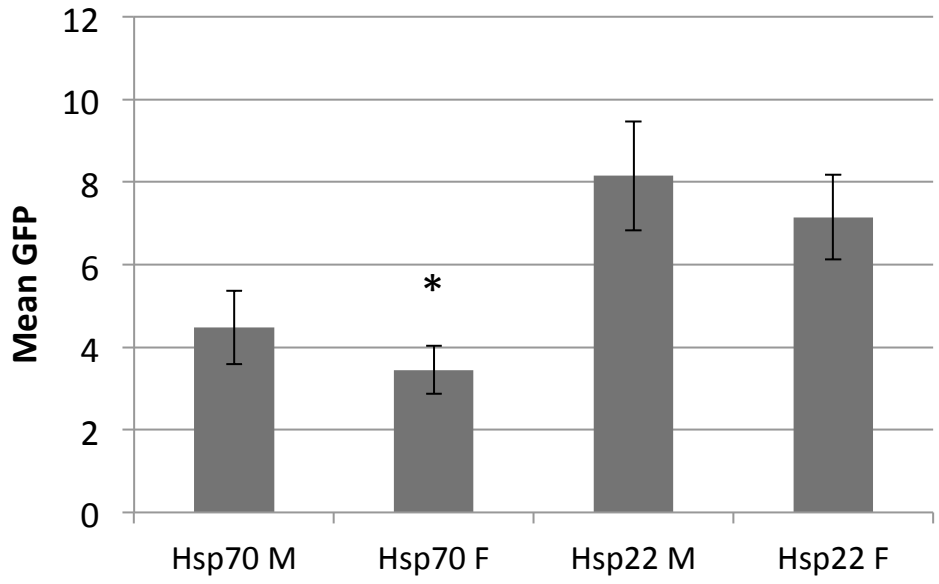

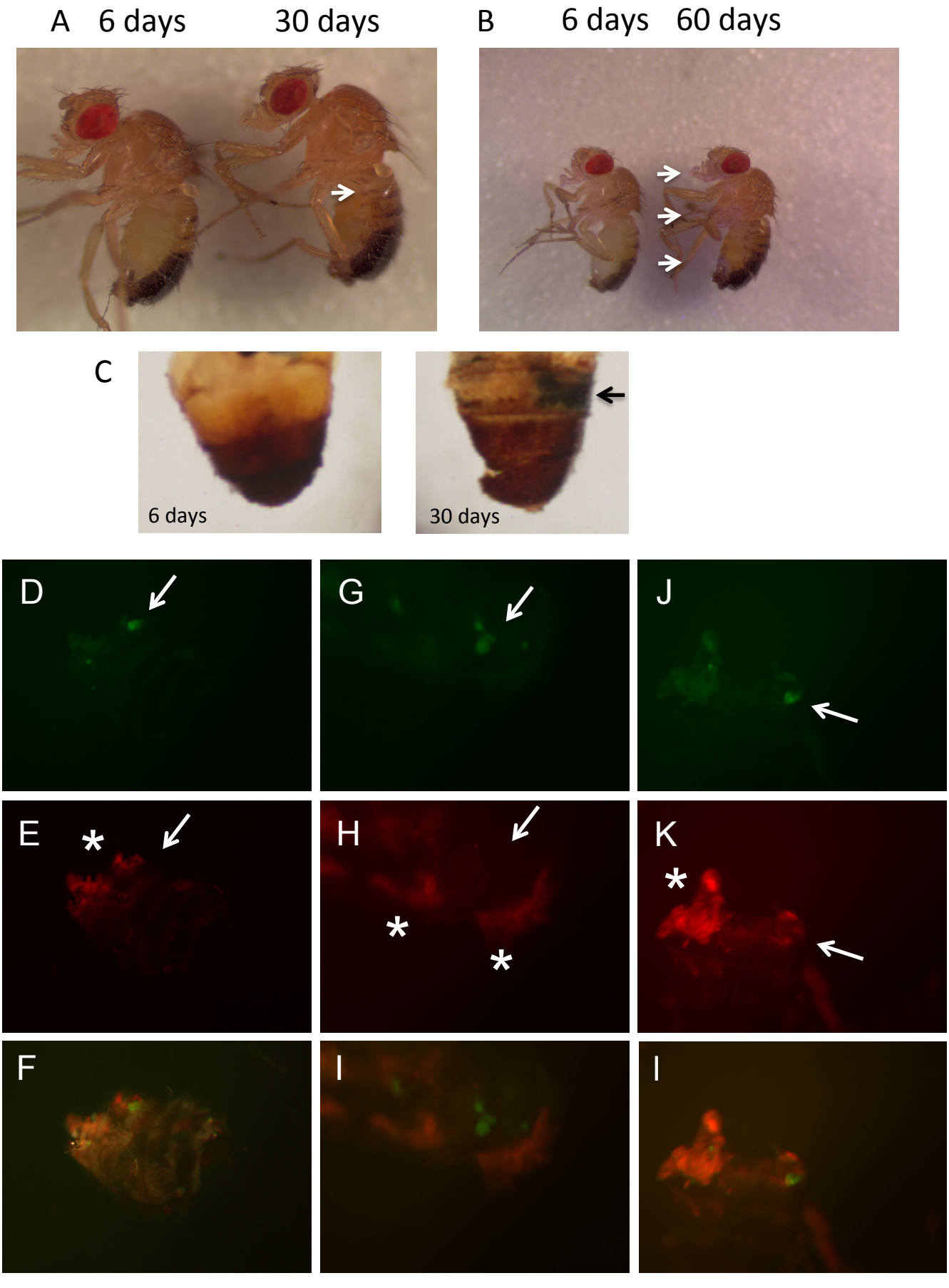
A 6 days 30 days
B 6 days 60 days
C
6 days
30 days
D
G
J
E
H
K
F
I
I

A

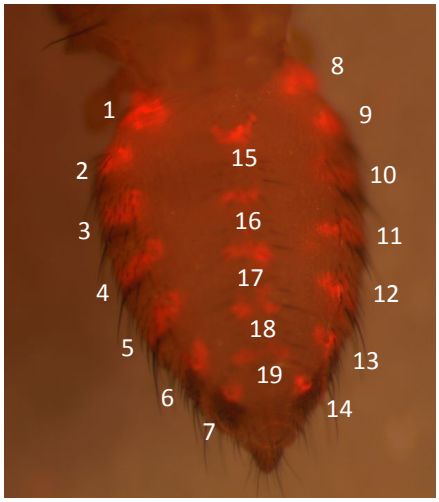
1
2
3
4
5
6
7
8
9
10
11
12
13
14
15
16
17
18
19

B

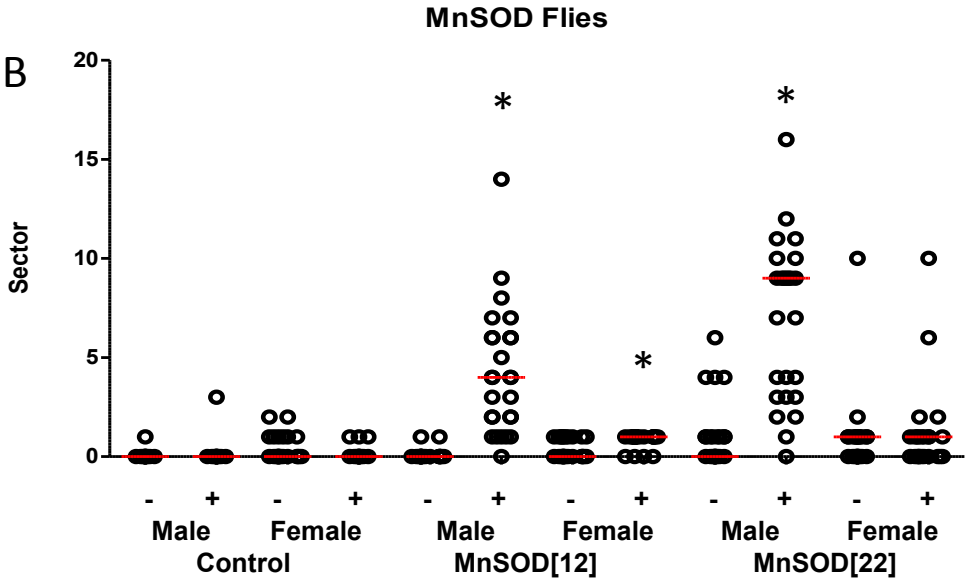
MnSOD Flies
Sector
20
15
10
5
0
- + - + - + - + - + - +
Male Female Male Female Male Female
Control MnSOD[12] MnSOD[22]

C

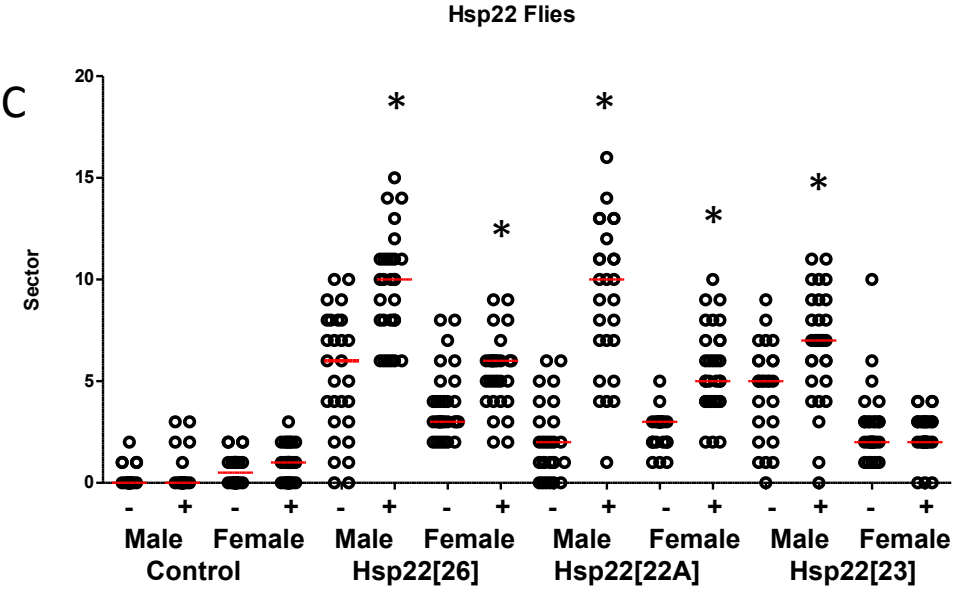
Hsp22 Flies
Sector
20
15
10
5
0
- + - + - + - + - + - + - + - +
Male Female Male Female Male Female Male Female
Control Hsp22[26] Hsp22[22A] Hsp22[23]